Growth of Free-Standing Polypyrrole Nanosheets at Air/Liquid Interface Using J-Aggregate of Porphyrin Derivative as in-Situ Template

ARTICLE *in* MACROMOLECULES · JUNE 2011

Impact Factor: 5.8 · DOI: 10.1021/ma2002849

Macromolecules

COMMUNICATION TO THE EDITOR

pubs.acs.org/Macromolecules

Growth of Free-Standing Polypyrrole Nanosheets at Air/Liquid Interface Using J-Aggregate of Porphyrin Derivative as in-Situ Template

Purushottam Jha, Shankar P. Koiry, Vibha Saxena, P. Veerender, Anil K. Chauhan, Dinesh K. Aswal,* and Shiv K. Gupta

Technical Physics Division, Bhabha Atomic Research Center, Mumbai 400 085, India

In recent years there is an increasing demand for the preparation of free-standing conducting polymer films as they can provide new opportunities in several applications such as understanding of fundamental mechanical or electrical properties, chemical or biosensors, ion-exchange membranes, organic electronics, polymeric batteries, artificial muscles, etc.[1,2] Among various conducting polymers, polypyrrole (PPy) is widely sought after due to its excellent stability under environmental conditions, good conductivity, and biocompatibility.[3] The free-standing PPy films have mainly been prepared by following two methods: (i) deposition onto the substrates by electropolymerization or spin-coating, followed by peeling the films off the substrates,[4−6] and (ii) segregating the PPy films prepared at liquid/liquid interface, i.e., chloroform/water along with $(NH_4)_2S_2O_8$, an oxidant.[7] The first approach either requires complicated equipment or suffers from damage during the transfer process, especially for nanometer-thick, large-area films. Similar problems occur while segregating the films grown at liquid/liquid interfaces. Very recently, ultrathin free-standing PPy films have also been prepared at an air/ionic liquid interface through interface oxypolymerization.[8] In this Communication, we report a novel one-pot fabrication strategy for the growth of free-standing PPy nanosheets. In our process spontaneously formed 5-(4- hydroxyphenyl)-10,15,20-triphenylporphyrin (TPPOH) J-aggregate films at the air/aqueous $FeCl_3$ interface acts as an in-situ template for the growth of PPy nanosheets.

Pyrrole (98%) was procured from Aldrich and distilled over calcium hydride under reduced pressure prior to use. Anhydrous $FeCl_3$ (LR grade) was purchased from Thomas Baker. The organic solvents used were of analytical grade, and Millipore water was used for washing and solution preparation. The TPPOH was synthesized using the procedure reported earlier.[9] The typical process employed for the growth of free-standing PPy films is as follows. In a beaker, 60 mL of 0.1 M aqueous $FeCl_3$ was taken, and in a steady state, a 200 μL solution consisting of 1 mM TPPOH and 0.01−1 M pyrrole prepared in dichloromethane (DCM) was slowly dropped using a micropipette. In addition, pure TPPOH and PPy films were prepared by dropping respectively 1 mM TPPOH or 0.1 M pyrrole solutions into $FeCl_3$. In all the cases, films were spontaneously formed at the air/$FeCl_3$ interface. Pure TPPOH films were formed within 5 min, while formation of pure PPy films took more than 20 min. All the films were mechanically strong and were lifted easily onto glass substrates. Prior to the characterization, all the films were thoroughly rinsed using Millipore water. Since TPPOH dissolves in DCM, therefore TPPOH/PPy bilayers were washed using DCM to obtain free-standing PPy films. The formation kinetics of TPPOH/PPy bilayer films was studied by lifting them onto glass substrates from an air/$FeCl_3$ interface after various time intervals and washing them using DCM. It was found that no residue was left on glass substrates for films lifted after $\leq$10 min, and it is only after this period, PPy films were left on the glass substrate. These results indicated that while TPPOH film is formed very quickly, the kinetics of interfacial polymerization of PPy is rather slow. The PPy films prepared without and with TPPOH would hereafter be referred as PPy-1 and PPy-2, respectively. These films were characterized by UV−vis spectroscopy (Jasco) and Fourier-transform infrared spectroscopy (Bruker 80 V). Surface morphology of the films was imaged using scanning electron microscopy (SEM) (TESCAN, TS5130MM). The electrical conductivity of the films was measured at room temperature using a Keithley meter (model 6487).

Figure 1a shows the photograph of the TPPOH/PPy bilayer formed at the air/$FeCl_3$ interface when a solution of 1 mM TPPOH + 0.1 M pyrrole was spread onto the surface of $FeCl_3$ solution. The blue color of the TPPOH/PPy bilayer is due to the characteristic color of TPPOH. The SEM image of PPy sheet (i.e., PPy-2 films) obtained after washing TPPOH/PPy bilayer in DCM is shown in Figure 1b. The thickness of the PPy-2 films was found in the range 120−140 nm, and the morphology, as shown in Figure 1c, consists of densely packed long PPy nanothreads. The thickness of the nanosheet however could be tailored by changing the pyrrole concentration. It was found that by increasing the pyrrole concentration from 0.01 to 1 M, the thickness of the nanosheet increases from 50 to 250 nm. However, at very high pyrrole concentrations, the SEM images, as shown in Figure 2, indicate that the film morphology turned to granular, which overlay nanosheets. On the other hand, the morphology of pure TPPOH and PPy-1 films, as shown in parts d and e of Figure 1, respectively, are remarkably different as compared to that of PPy-2 films. TPPOH films exhibit highly dense morphology that consists of square (size: ~2 μm) and lamellar structure, whereas the morphology of PPy-1 film is porous and granular in nature. In the following we demonstrate that the dense morphology of PPy-2 films as compared to that of PPy-1 films arise due to a template action of TPPOH films.

Received: February 8, 2011
Revised: April 24, 2011
Published: May 26, 2011

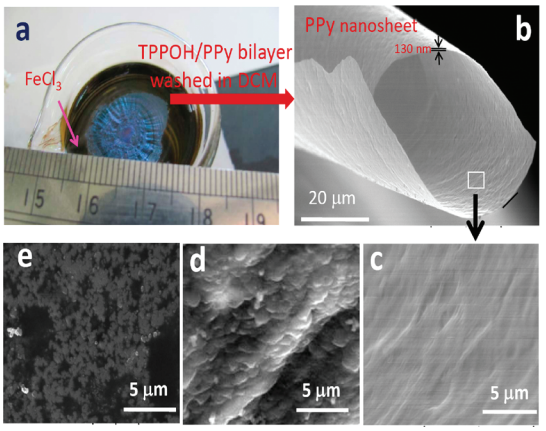

Figure 1. (a) Photograph of the TPPOH/PPy bilayer formed at the air/$FeCl_3$ interface film prepared using 0.1 M PPy solution. SEM images: (b) PPy-2 film obtained after washing TPPOH/PPy bilayer in DCM; (c) magnified image of PPy-2 film; (d) J-aggregate film of TPPOH; and (e) PPy-1 films that is formed without TPPOH.

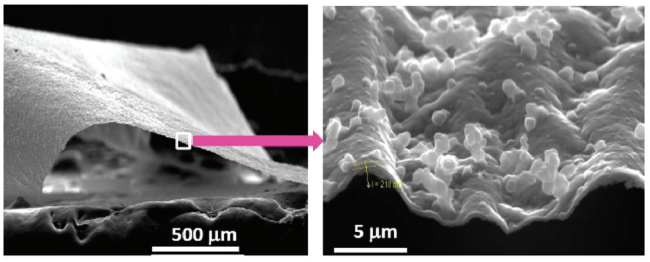

Figure 2. SEM images of PPy-2 film prepared using 1 M PPy solutions.

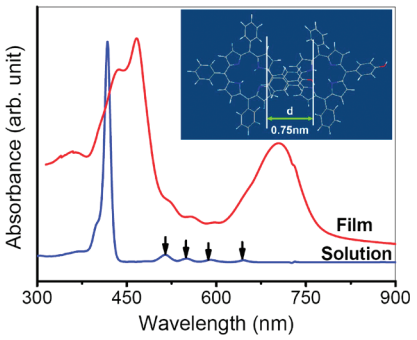

Figure 3. UV−vis spectra of TPPOH solution in dichloromethane and TPPOH film formed at air/aqueous $FeCl_3$ interface. Inset shows a schematic of the J-aggregate formation, where *d* is the slipping distance.

First of all, we investigate the origin of dense and lamellar morphology of pure TPPOH films (see Figure 1d). Aggregation is a well-known phenomenon for molecules with a flat and extended π-electron systems like TPPOH, in which monomeric units stack into edge-to-edge (J-aggregate) and/or face-to-face (H-aggregate) configurations.[10] In order to investigate the type of aggregation in TPPOH, we have recorded the transmission absorption spectra of the TPPOH films and TPPOH monomer solution (prepared by dissolving TPPOH in DCM), and the results are shown in Figure 3. It is seen that the absorption spectra for TPPOH film is relatively broad as compared to that of

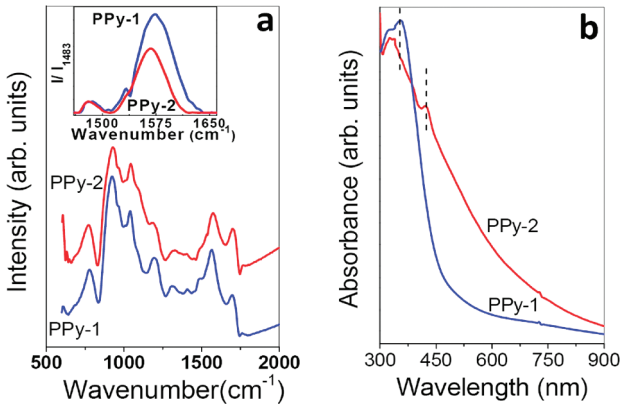

Figure 4. (a) FTIR spectra of PPy-1 and PPy-2 films. Inset shows the FTIR spectra in the 1450−1650 cm^{-1} region with intensity normalized with respect to 1483 cm^{-1} peak. (b) UV/vis spectra for PPy-1 and PPy-2 films.

TPPOH solution, suggesting the occurrence of an incoherent interaction in the surroundings of the dense film. For TPPOH film, the Soret band appears at 466 nm (along with a shoulder at 436 nm) as compared to the 418 nm observed for the free base monomers. Similarly, the weak Q-bands at 514, 549, 588, and 694 nm observed for monomers are replaced by an intense single band at 705 nm. Observed red-shift of both Soret and Q bands confirms the formation of J-aggregates (note: H-aggregation results in the blue-shift).[11] In the case of TPPOH film, the J-aggregation possibly occurs due to hydrogen bonding between the hydroxyl group of one molecule (attached at para position of phenyl ring) and N−H bonds at porphyrin core of adjacent molecule, as schematically shown in the inset of Figure 3. The presence of strong high-energy absorption shoulder of the B-band (i.e., at 436 nm)—usually assigned to the orthogonal transition dipole to the aggregation axis—suggests that the slipping distance (*d*) is quite short.[11] Theoretically estimated value of *d* in the case of TPPOH is found to be 0.75 nm. Therefore, the J-aggregation of TPPOH with small slipping distance can yield lamellar structure as experimentally observed in Figure 1d. As mentioned earlier, the TPPOH films are formed within 5 min, and this is attributed to the presence of Fe^{3+}, which is known to induce J-aggregation at a very fast rate.[12] Therefore, it is established that the J-aggregation of TPPOH films occurs at a very fast rate. Considering the experimental fact that formation of pure PPy film (i.e., PPy-1 formed without TPPOH) takes about 20 min, it is apparent that in the case of TPPOH/PPy bilayer the quickly formed TPPOH film at air/$FeCl_3$ interface acts as an in-situ template for the growth of PPy nanosheets. The template action is obtained as the N−H group of pyrrole rings forms hydrogen bonding with porphyrin core of the J-aggregates, which provides directionality for pyrrole polymerization in the form of nanothreads, as observed in Figure 1c. Closely packed nanothreads leads to the formation of a mechanically strong PPy nanosheets. In order to further confirm that J-aggregate film of TPPOH only acts as template and does not incorporate into PPy-2 films, we have recorded the FTIR spectra, as shown in Figure 4. It has been found the FTIR spectrum of the PPy-2 nanosheets is almost identical to that of PPy-1 films, which exhibit all characteristic peaks of polypyrrole,[13−15] i.e., symmetric (1567 cm^{-1}) and antisymmetric (1483 cm^{-1}) ring stretching modes, C−N (1313 cm^{-1}), C−C (1408 cm^{-1}), C−H in-plane bending

dx.doi.org/10.1021/ma2002849 |*Macromolecules* 2011, 44, 4583–4585

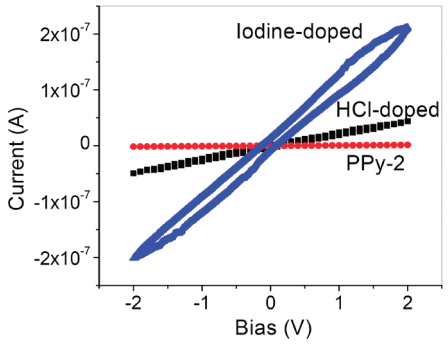

Figure 5. Current−voltage characteristics recorded for the PPy-2 films in pristine state and after doping with iodine and HCl vapors for 1 h.

(1196 cm^{-1}), polypyrrole main chain (1040 cm^{-1}) and ring bending vibrations (778 and 924 cm^{-1}). The absence of peak corresponding to OH—a characteristic of TPPOH—confirms that TPPOH does not incorporate into the PPy-2 films.

Our experimental results show that PPy-2 films are superior to PPy-1 films in terms of improved conjugation length. First evidence to this comes from the FTIR intensity ratio (I_{1567}/I_{1483}), which is reported to be inversely proportional to the conjugation length.[16] The data presented in the inset of Figure 4a, therefore, clearly show an enhanced conjugation for PPy-2 films, which is in accordance with their dense morphology. The second confirmation of improved conjugation length comes from the UV−vis spectra, as shown in Figure 4b. PPy-2 films shows absorption peak at 424 nm (corresponding to the $\pi-\pi^*$ transition of the PPy chain[17]), while for PPy-1 films the peak occurs at 355 nm. A red-shift in the absorption peak observed for PPy-2 films confirms their enhanced conjugation length. Another notable feature of the UV/vis spectra is the absence of broad absorption peak at around 600 nm, which has been observed in doped PPy due to the polaron transition.[17] This indicates that both PPy-1 and PPy-2 films are undoped. This is further confirmed by the conductivity measurements, which were found to be quite low, i.e., 5×10^{-6} and 3×10^{-5} S/cm for PPy-1 and PPy-2 films, respectively. Typical current−voltage characteristics recorded for PPy-2 films in pristine state and after exposing to iodine and HCl vapors for 1 h each are shown in Figure 5. It has been found that the conductivity improves by 30 times on exposing to HCl and ∼150 times on exposure to iodine, clearly indicating that conductivity of PPy-2 films can be tailored by appropriate doping. The investigation of charge transport properties of Ppy-2 films as a function of doping level and temperature is underway and will be reported later. Most importantly, PPy nanosheets showed no change in conductivity when kept in air for more than 6 months, indicating their stability in air.

In conclusion, we have demonstrated a novel strategy for the one-pot fabrication of free-standing PPy-nanosheets by dropping 200 μL solution, consisting of 1 mM porphyrin derivative (TPPOH) and 0.01−1 M pyrrole (Py), to 0.1 M aqueous $FeCl_3$ solution kept in a beaker. TPPOH/PPy bilayer is found to form spontaneously at the air/$FeCl_3$ interface, which after washing in dichloromethane yielded in free-standing PPy-nanosheets. UV/vis and FTIR studies show that TPPOH quickly forms J-aggregate films at the air/$FeCl_3$ interface, which acts as in-situ template for the growth of PPy-nanosheets. The advantage of our method is that it is very simple and does not require sophisticated instruments for obtaining the free-standing polypyrrole films with dense morphology. In fact, this approach can be used for preparing nanosheets of other conducting polymers as well.

AUTHOR INFORMATION

Corresponding Author

*E-mail: dkaswal@yahoo.com; Ph: +91-22-25593838; Fax: +91-22-25505296.

ACKNOWLEDGMENT

This work is supported by "DAE-SRC Outstanding Research Investigator Award" (2008/21/05-BRNS) and "Prospetctive Research Funds" (2008/38/02-BRNS) granted to D.K.A.

REFERENCES

(1) (a) Cheng, W.; Campolongo, M. J.; Tan, S. J.; Luo, D. *Nano Today* **2009**, *4*, 482–493. (b) Zhang, L.; Hendel, R. A.; Cozzi, P. G.; Regen, S. L. *J. Am. Chem. Soc.* **1999**, *121*, 1621–1622. (c) Uozumi, Y.; Yamada, Y. M. A.; Beppu, T.; Fukuyama, N.; Ueno, M.; Kitamori, T. *J. Am. Chem. Soc.* **2006**, *128*, 15994–15995. (d) Yang, H.; Coombs, N.; Sokolov, I.; Ozin, G. A. *Nature* **1996**, *381*, 589–592.

(2) (a) Yang, H. H.; Zhang, S. Q.; Tan, F.; Zhuang, Z. X.; Wang, X. R. *J. Am. Chem. Soc.* **2005**, *127*, 1378–1379. (b) Ramanathan, K.; Bangar, M. A.; Yun, M.; Chen, W.; Myung, N. V.; Mulchandani, A. *J. Am. Chem. Soc.* **2005**, *127*, 496–497. (c) Berdichevsky, Y.; Lo, Y. H. *Adv. Mater.* **2006**, *18*, 122–125.

(3) Ramanaviciene, A.; Ramanavicius, A. *Crit. Rev. Anal. Chem.* **2002**, *32*, 245–252.

(4) Shi, G.; Jin, S.; Xue, G.; Li, G. *Science* **1995**, *267*, 994–996.

(5) Otero, T. F.; Ariza, M. J. *J. Phys. Chem. B* **2003**, *107*, 13954–13961.

(6) Sutar., D.; Aswal, D. K.; Gupta, S. K.; Yakhmi, J. V. *Indian J. Pure Appl. Phys.* **2007**, *45*, 354–357.

(7) Lu, Y.; Shi, G.; Li, C.; Liang, Y. J. *Appl. Polym. Sci* **1998**, *70*, 2169–2172.

(8) Wang, D.; Li, Y. X.; Shi, Z.; Qin, H. L.; Wang, L.; Pei, X. F.; Jin., J. *Langmuir* **2010**, *26*, 14405–14408.

(9) Koiry, S. P.; Aswal, D. K.; Chauhan, A. K.; Saxena, V.; Nayak, S. K.; Gupta, S. K.; Yakhmi, J. V. *Chem. Phys. Lett.* **2008**, *453*, 68–73.

(10) Michihiro, S.; Norifumi, F.; Seiji, S. *J. Am. Cem. Soc.* **2005**, *127*, 4164–4165.

(11) Okada, S.; Segawa, H. *J. Am. Chem. Soc.* **2003**, *125*, 2792–2796.

(12) Ma, H. L.; Jin, W. J. *Spectrochim. Acta, Part A* **2008**, *71*, 153–160.

(13) Cho, G.; Bing, M. F.; Daniel, T.; Lee, J. S.; Shul, Y. G. *Langmuir* **2001**, *17*, 456–461.

(14) Jang, K. S.; Lee, H.; Moon, B. *Synth. Met.* **2004**, *143*, 289–294.

(15) Davidson, R. G.; Turner, T. G. *Synth. Met.* **1995**, *72*, 121–125.

(16) Menon, V. P.; Lei, J.; Martin, C. R. *Chem. Mater.* **1996**, *8*, 2382–2390.

(17) Kim, D. Y.; Lee, J. Y.; Moon, D. K.; Kim, C. Y. *Synth. Met.* **1995**, *69*, 471–474.